Electronic Supplementary Material (ESI) for Analyst.

Electronic Supplementary Information

Investigating C=C positions and hydroxylation sites in lipids using Paternò-Büchi functionalization mass spectrometry

Patrick Esch[a] and Sven Heiles[a]*

[a] *Institute of Inorganic and Analytical Chemistry, Justus Liebig University Giessen, 35392 Giessen, Germany*

*Address correspondence to Dr. Sven Heiles:
Institute of Inorganic and Analytical Chemistry
Justus Liebig University Giessen
Heinrich Buff Ring 17
35392 Giessen, Germany
Phone: +49 641 99 34807
e-mail: sven.heiles@anorg.chemie.uni-giessen.de

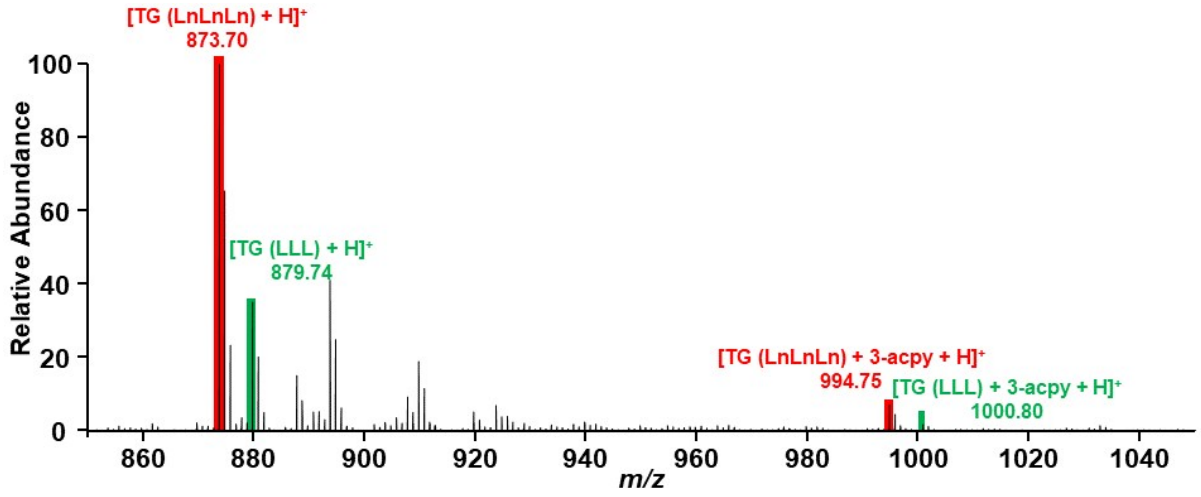

Figure S1. Overview spectrum of a solution containing 1 µM/L TG (LnLnLn), 1 µM/L TG (LLL) and 10 µM/L 3-acpy in MeOH and 1% formic acid after UV irradiation.

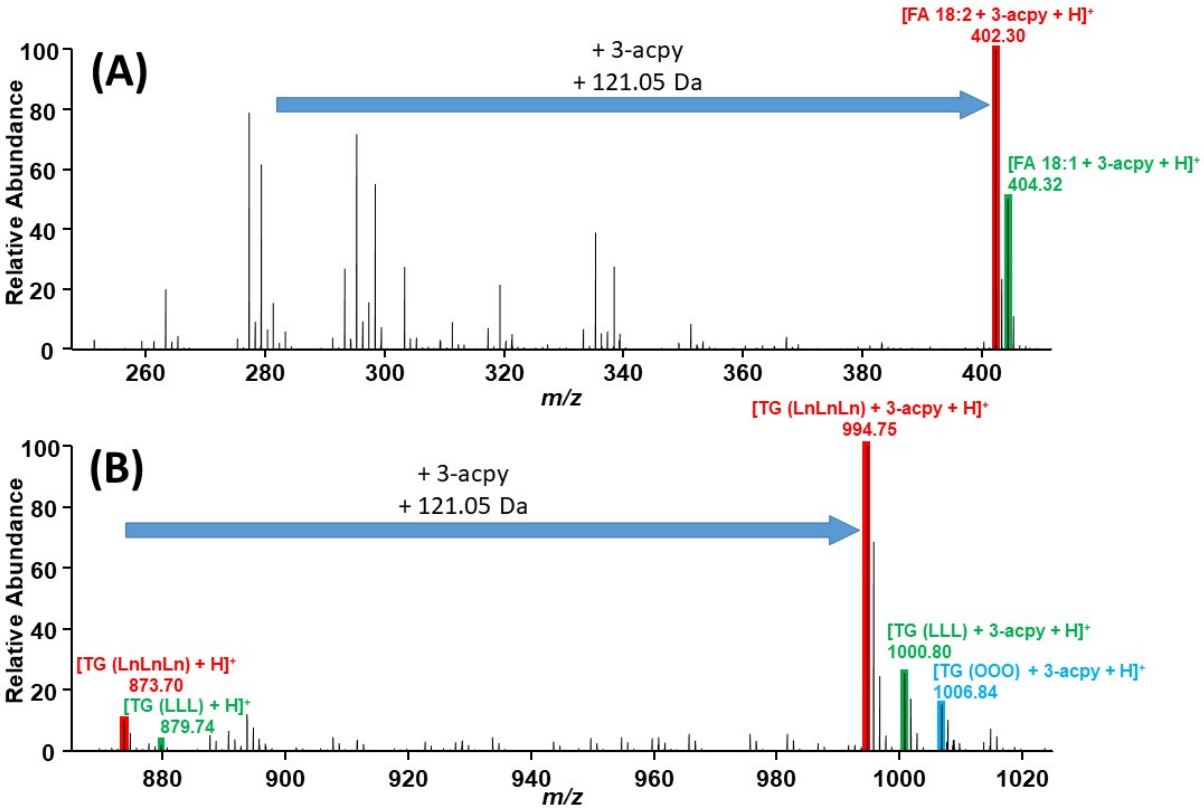

Figure S2. Overview spectra of a MeOH solution containing 1 mM/L 3-acpy and 1 µM/L **(A)** FA 18:1, FA 18:2 as well as **(B)** TG (OOO), TG (LLL) and TG (LnLnLn). **(A)** Overview mass spectrum of fatty acids after PB reactions. The unfunctionalized $[FA + H]^+$-ions were not detected and the mass shift of +121.05 Da is indicated with respect to hypothetical $[FA + H]^+$-ions. **(B)** Overview mass spectrum of TGs after PB reactions.

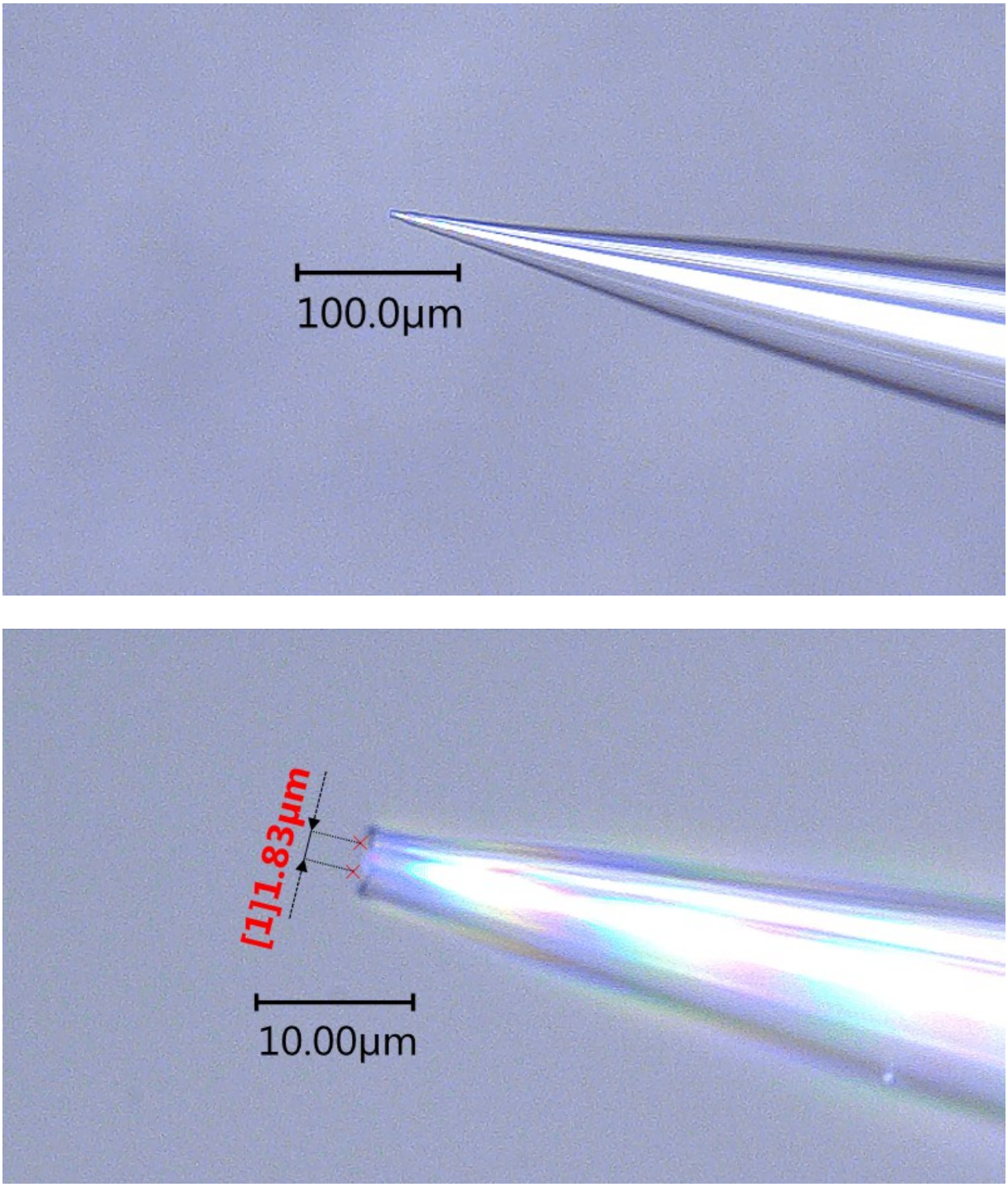

Figure S3. Microscopic image of a nanoESI emitter tip with an inner diameter of about 1.8 µm.

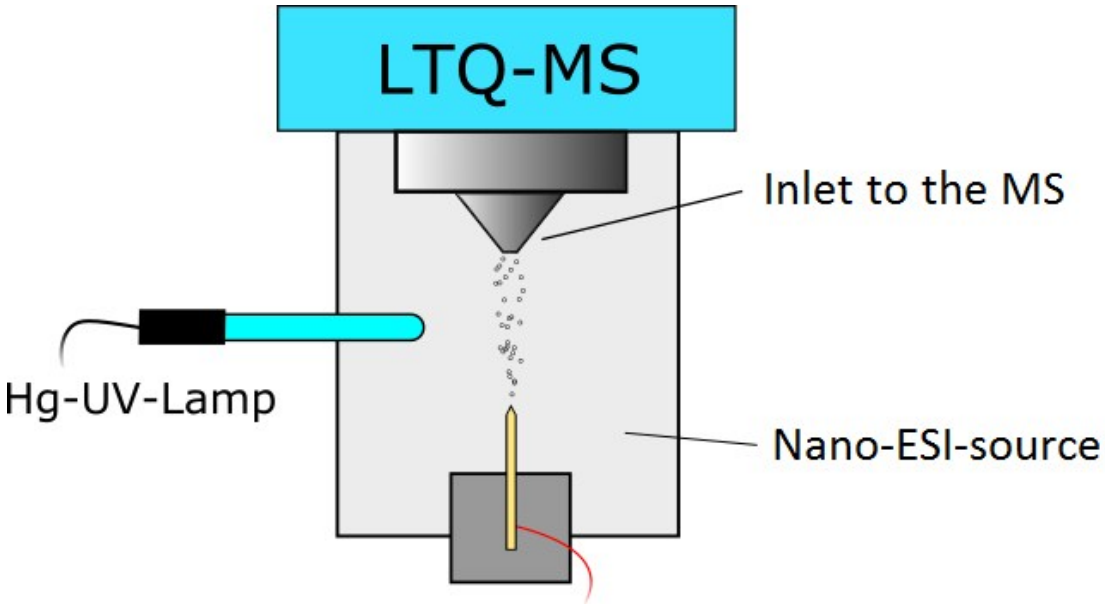

Figure S4. Scheme of the experimental nESI setup. The brass shielding of the UV lamp is omitted for clarity.

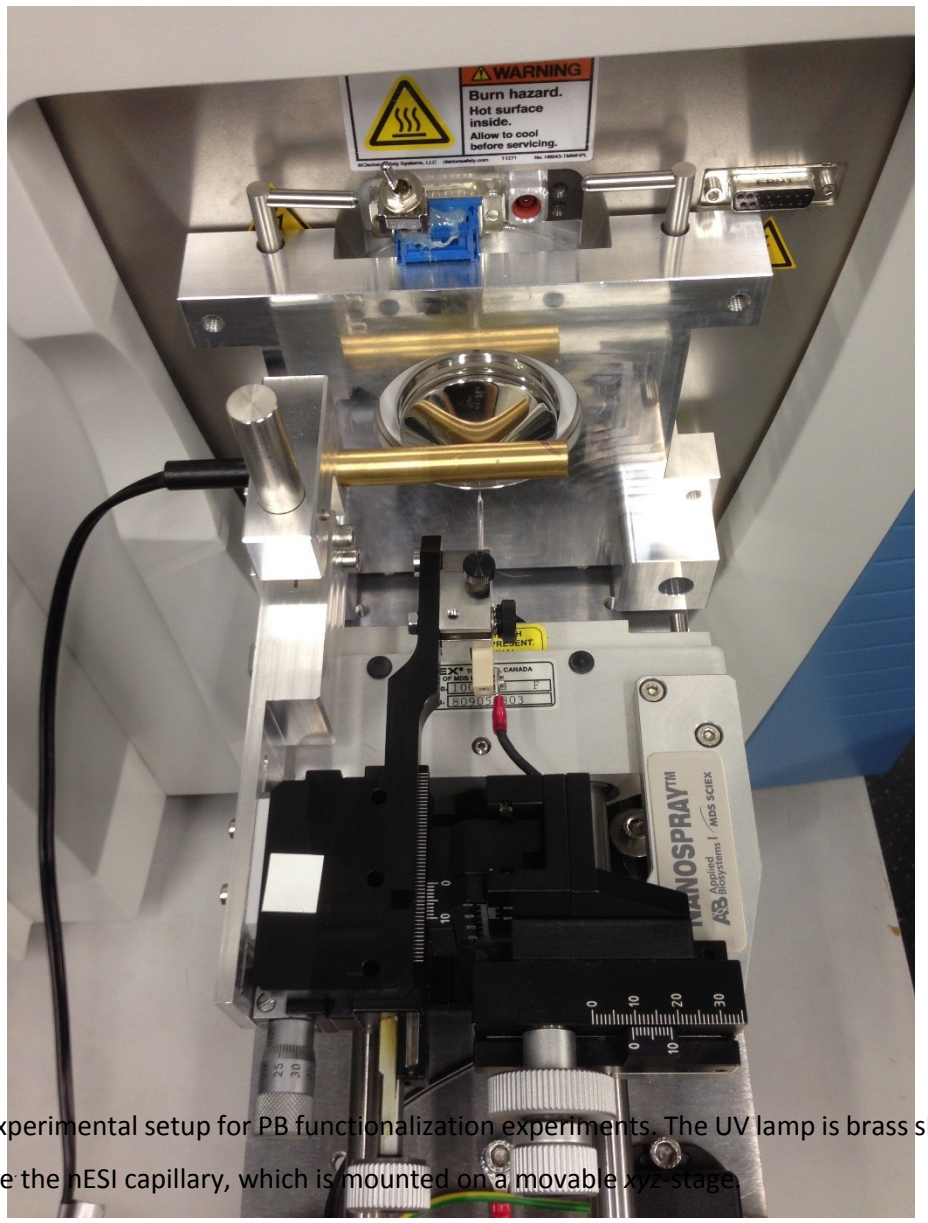

Figure S5. Experimental setup for PB functionalization experiments. The UV lamp is brass shielded and placed above the nESI capillary, which is mounted on a movable *xyz*-stage.

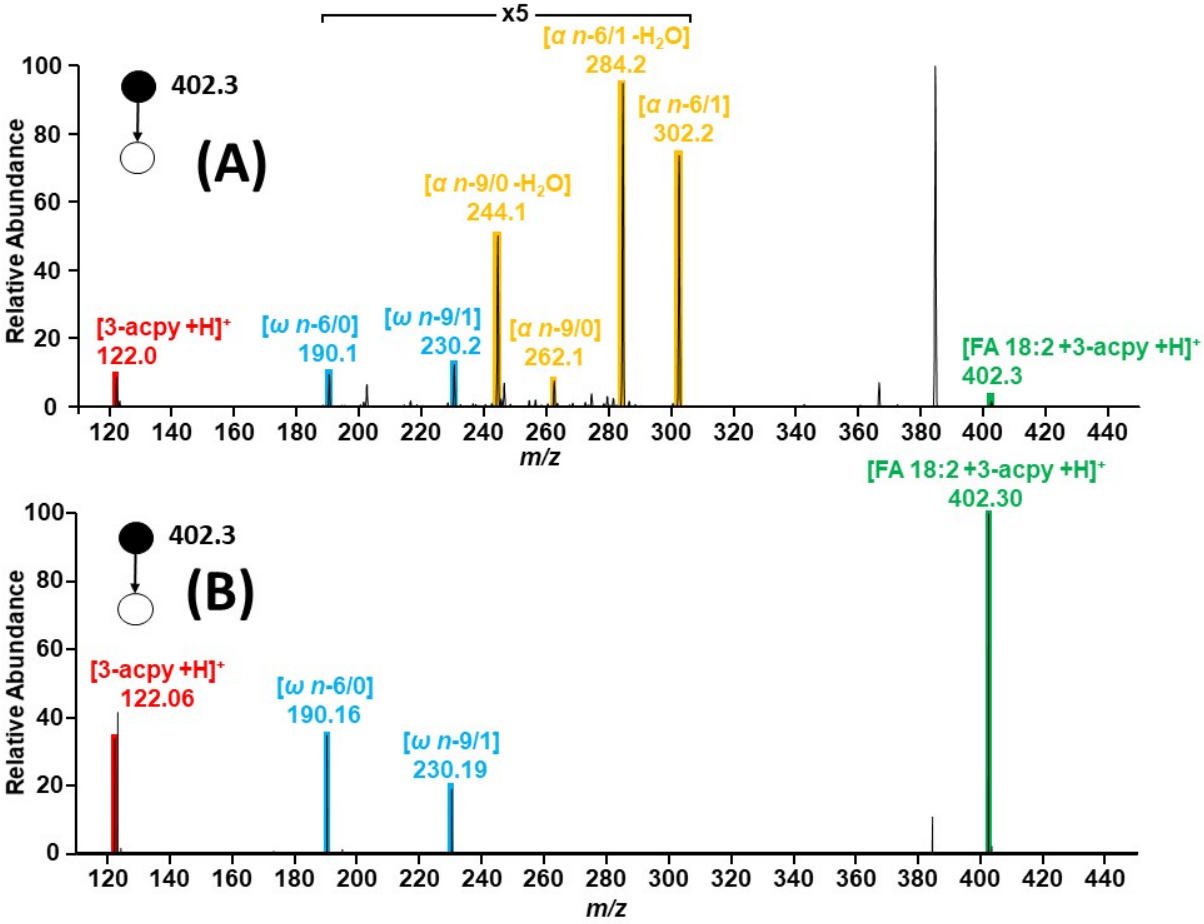

Figure S6. **(A)** CID-MS^2 and **(B)** HCD-MS^2 spectra of PB-functionalized linoleic acid (FA 18:2 *n*-6, *n*-9).

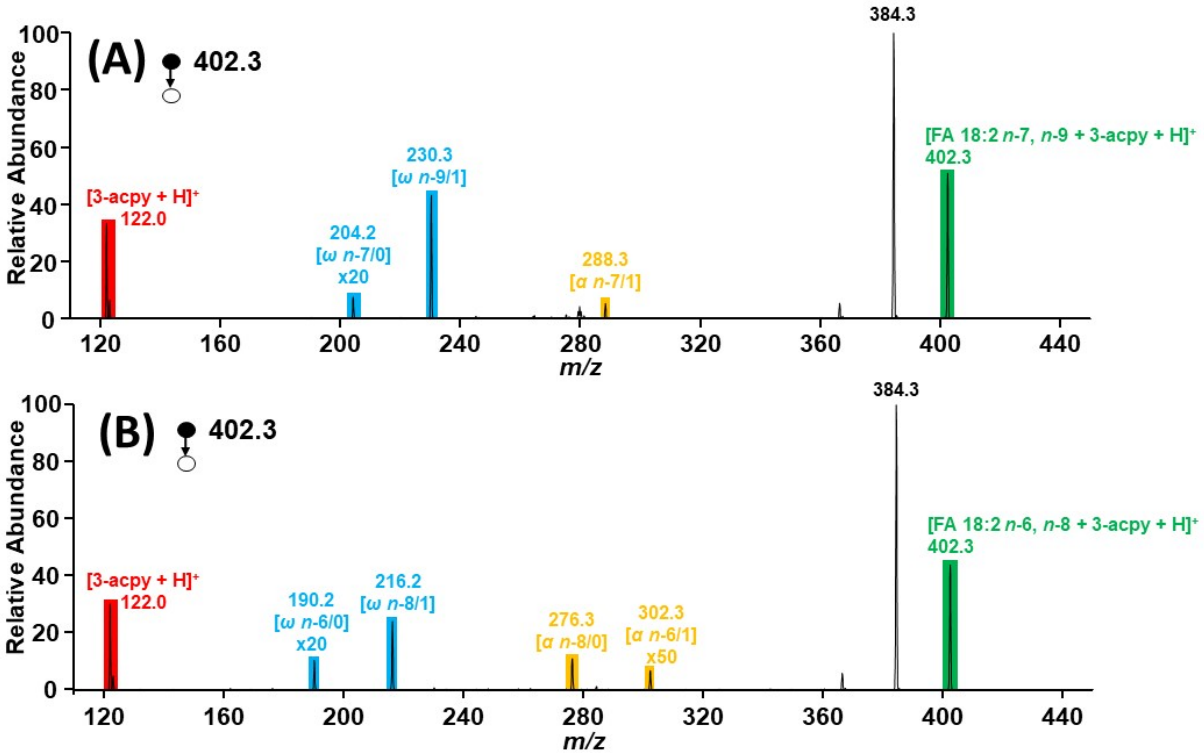

Figure S7. **(A)** CID-MS^2 spectrum of functionalized FA 18:2 *n*-7, *n*-9. **(B)** CID-MS^2 spectrum of functionalized FA 18:2 *n*-6, *n*-8.

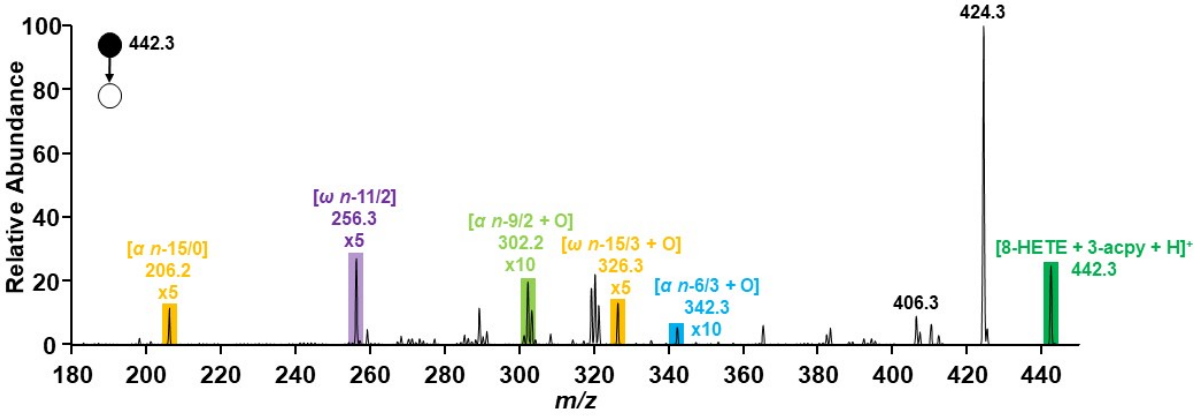

Figure S8. CID-MS^2 spectrum of PB-functionalized 8-HETE.

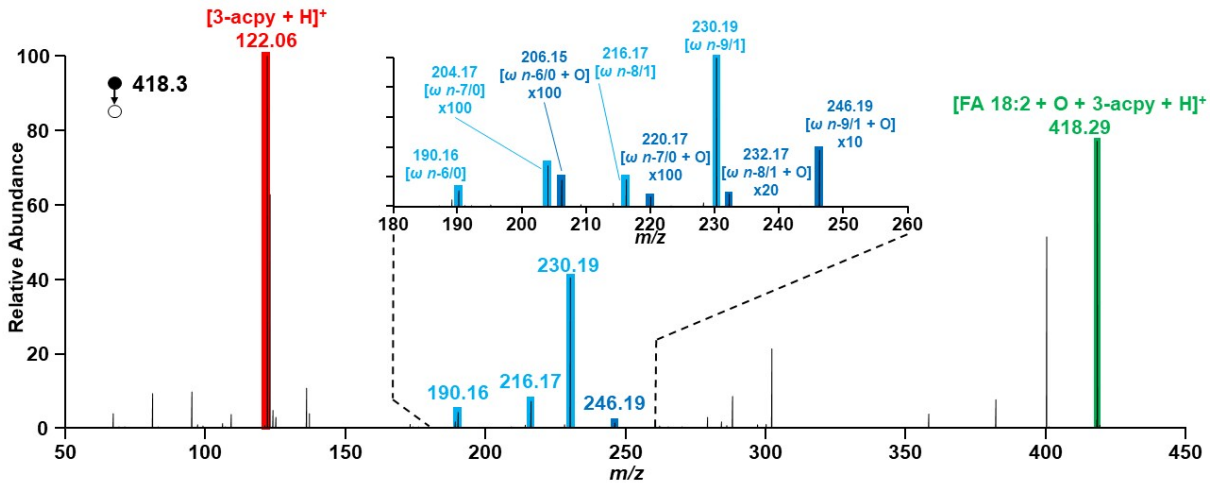

Figure S9. MS^2 spectrum of PB-functionalized linoleic acid standard oxidized under ambient conditions for 69 h. *ω*-ions for *n*-6, *n*-7, *n*-8 and *n*-9 were detected as well as their corresponding oxidized form.

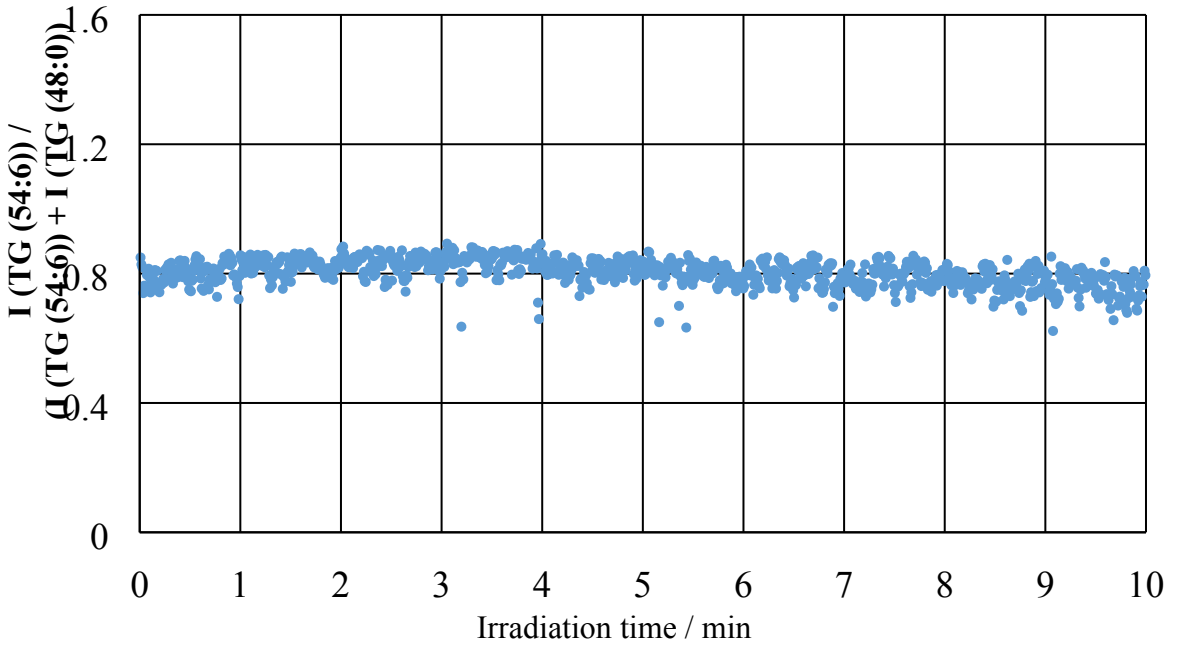

Figure S10. Signal intensity of protonated TG (18:2/18:2/18:2) relative to the protonated TG (16:0/16:0/16:0) signal as a function of UV irradiation time.

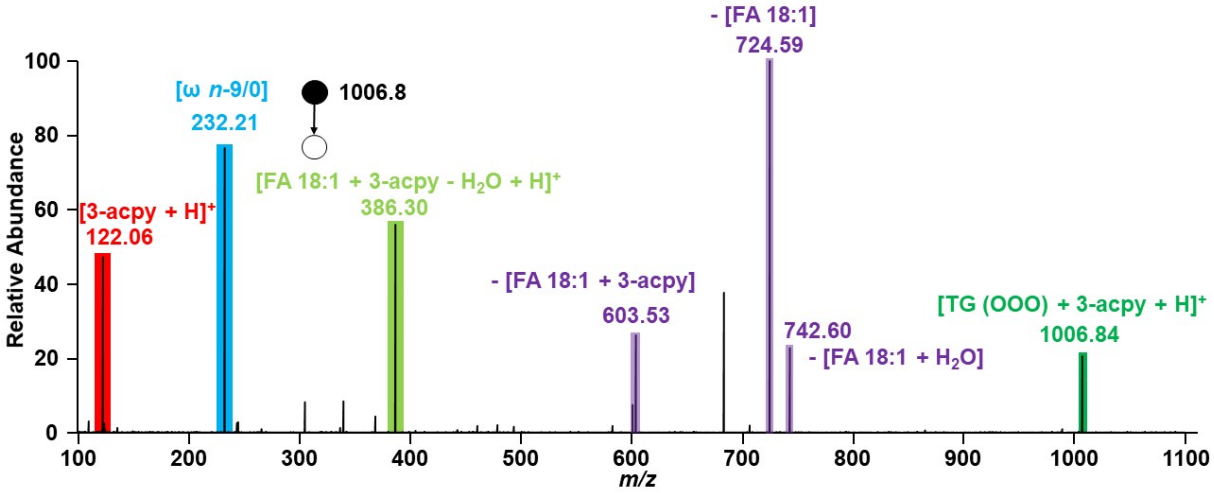

Figure S11. PB MS/MS spectrum of TG (OOO) with *m/z* 1006.8.

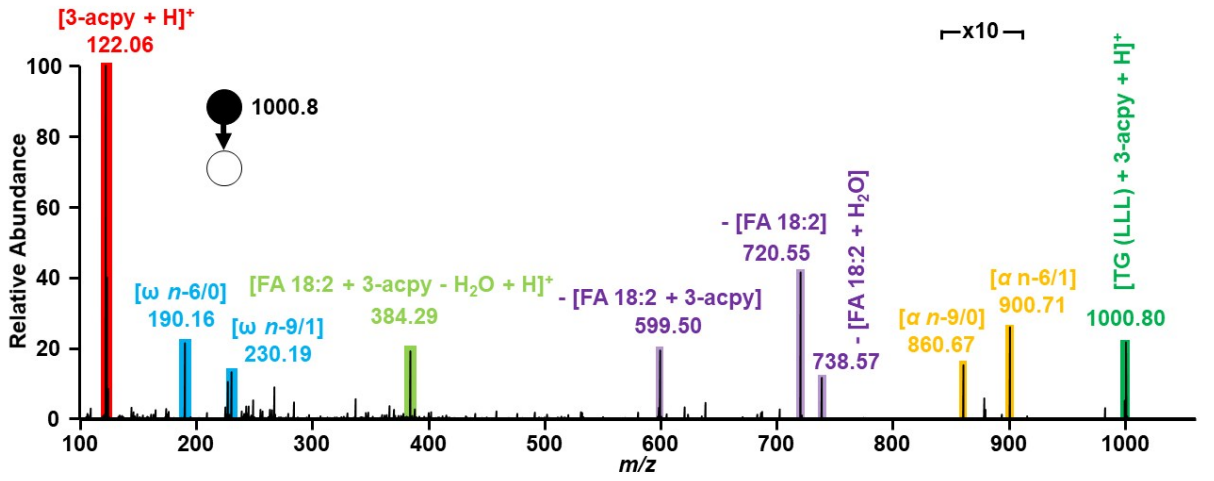

Figure S12. PB MS/MS spectrum of TG (LLL) with *m/z* 1000.80.

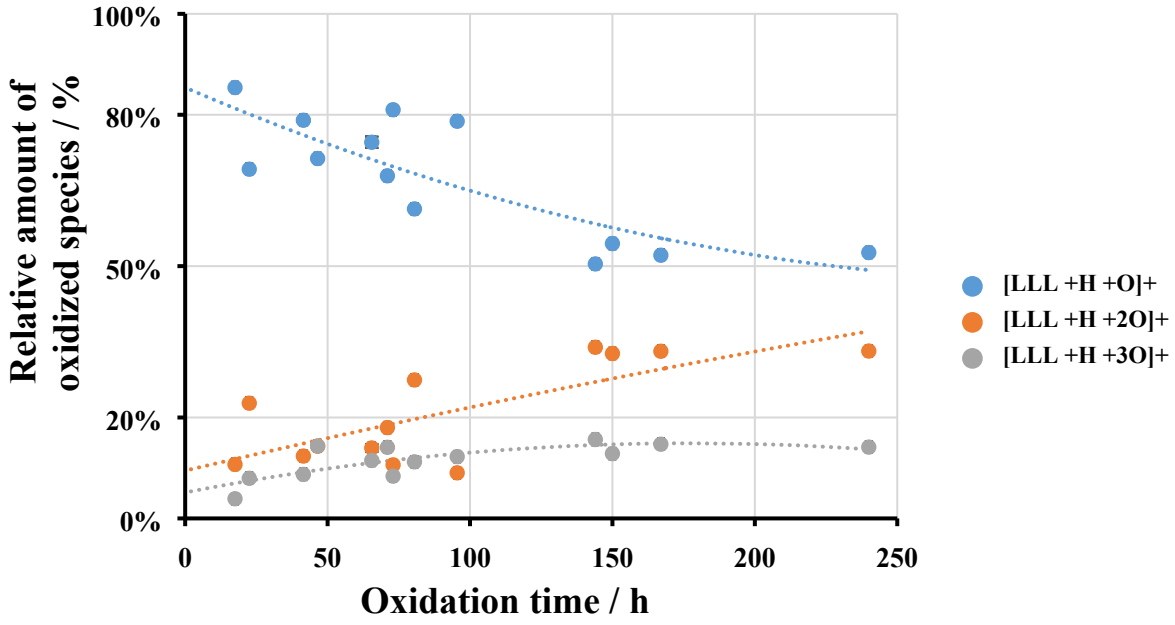

Figure S13. Time-dependent relative abundance of mono-, di- and tri-oxidized TG (LLL) species. Lines are second-degree polynomials and serve as guide to the eye.

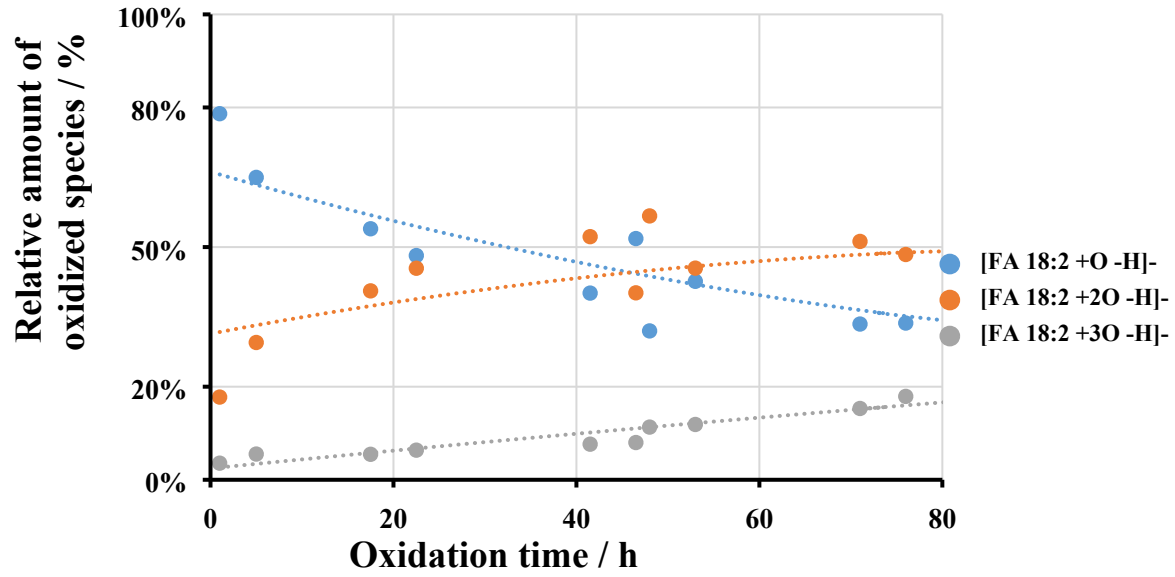

Figure S14. Time-dependent relative abundance of mono-, di- and tri-oxidized FA 18:2 species. Lines are second-degree polynomials and serve as guide to the eye.

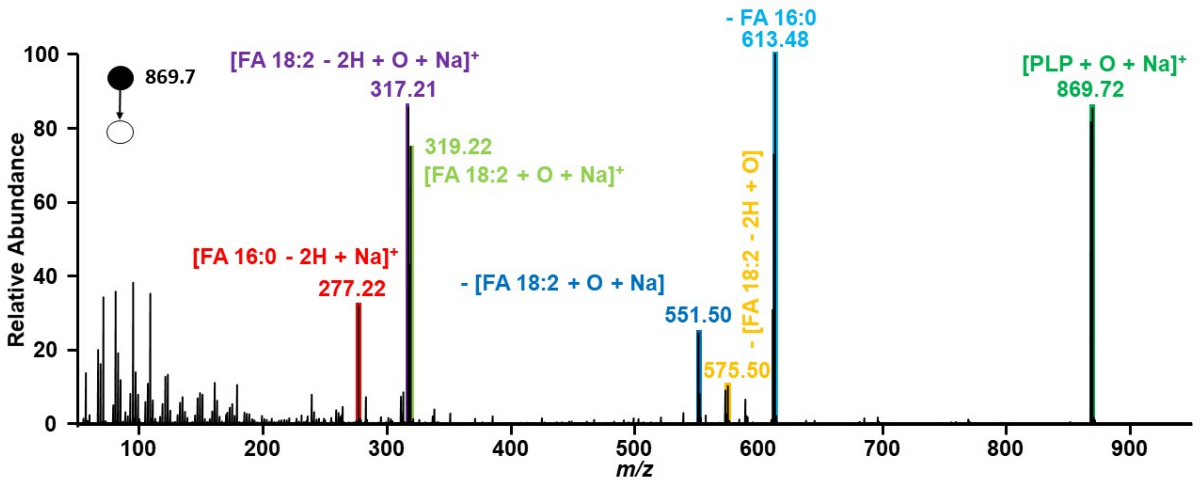

Figure S15. MS/MS spectrum of [PLP + O + Na]$^+$ with *m/z* 869.

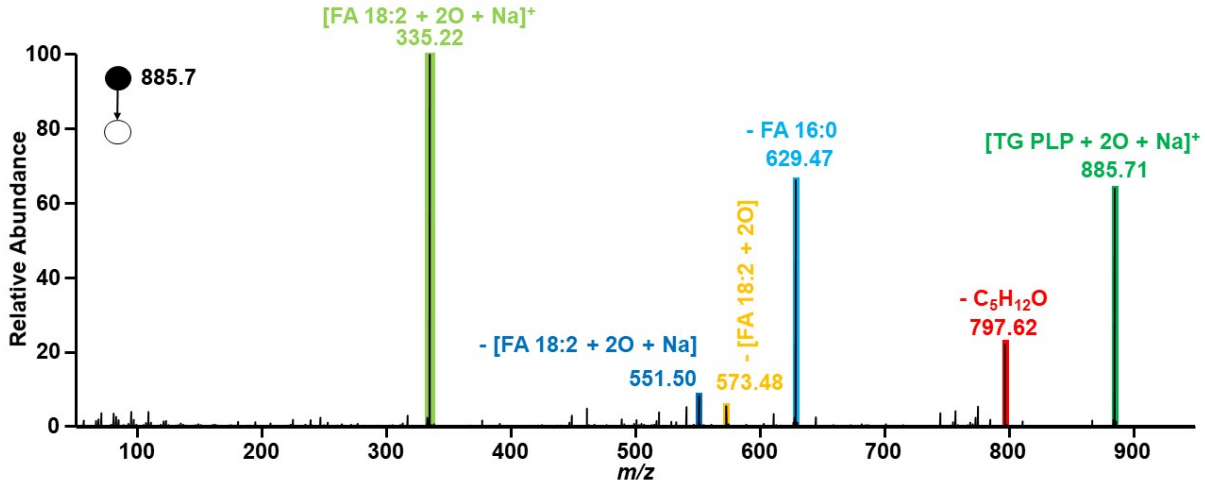

Figure S16. MS/MS spectrum of [PLP + 2O + Na]$^+$ with *m/z* 885.

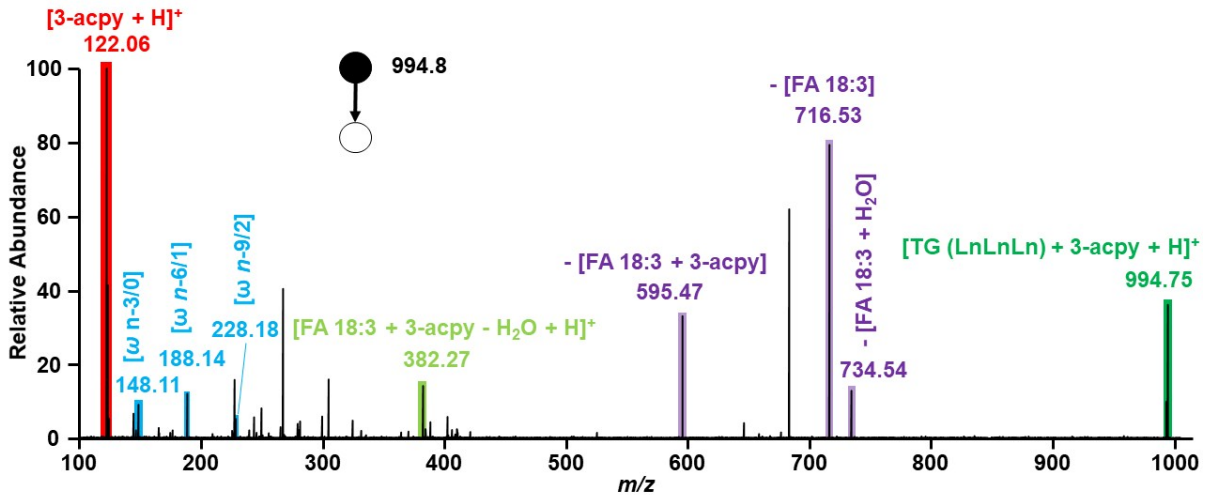

Figure S17. PB MS/MS spectrum of TG (LnLnLn) with *m/z* 994.75.

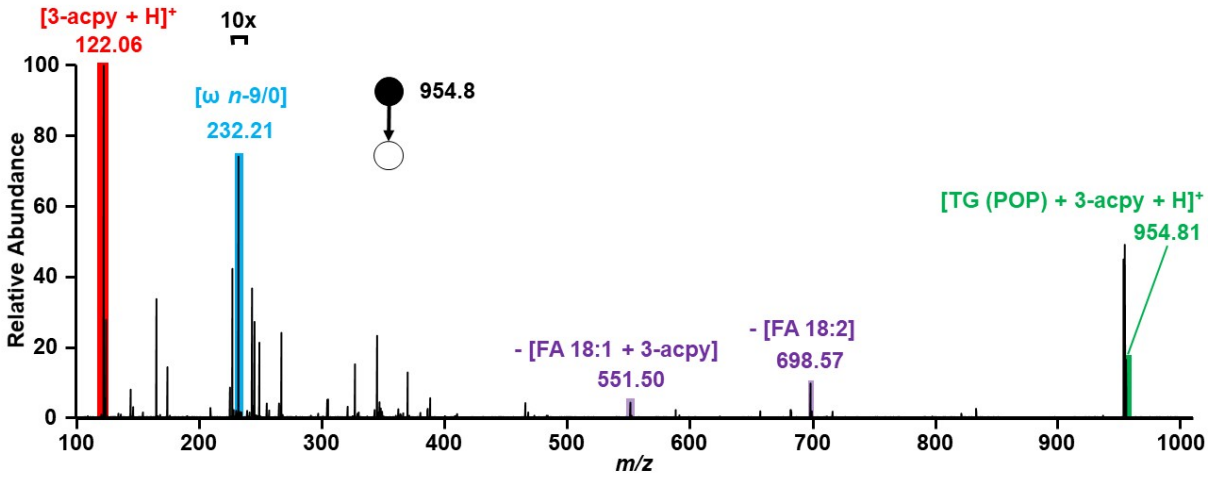

Figure S18. PB MS/MS spectrum of TG (POP) with *m/z* 954.81.

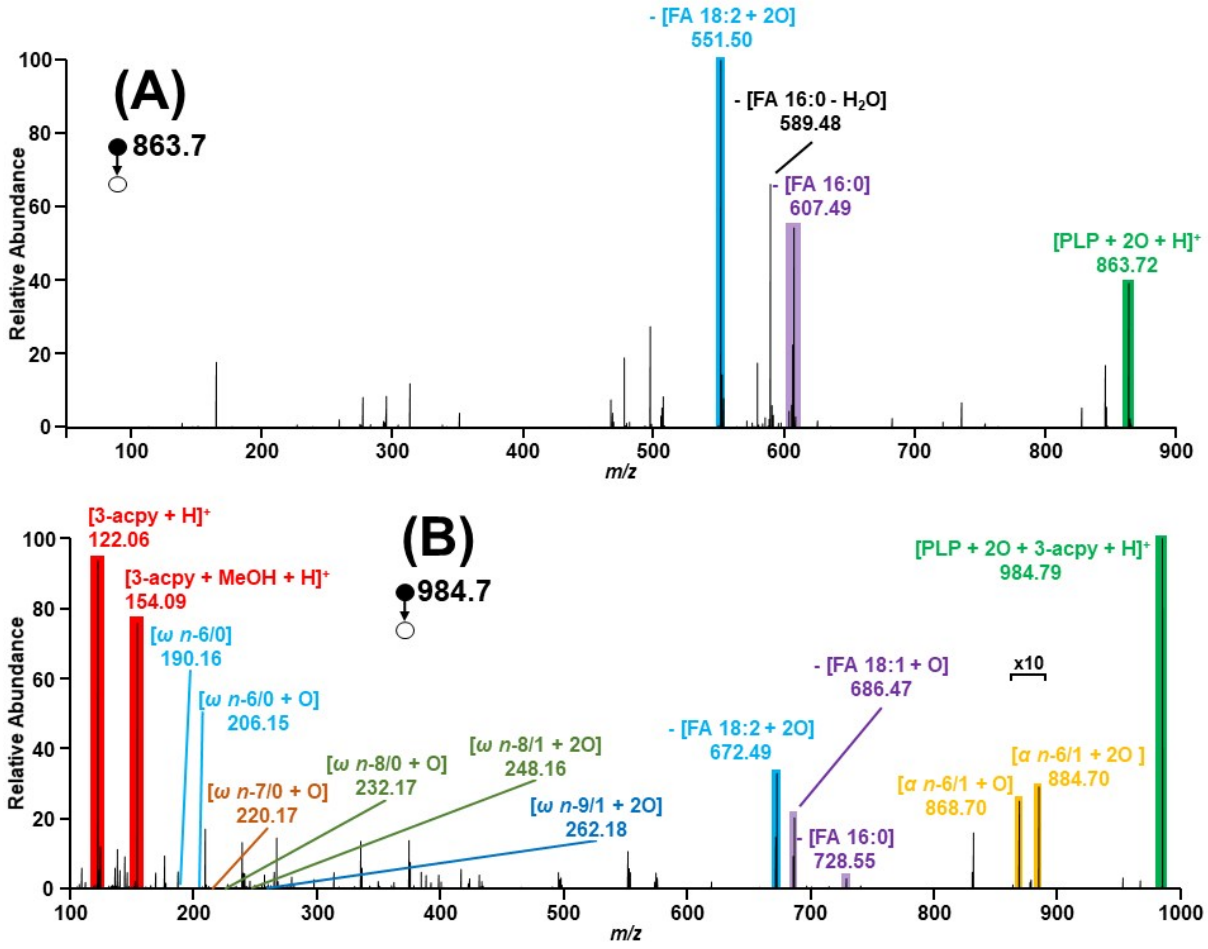

Figure S19. (A) MS/MS spectrum of di-oxidized, non-functionalized [PLP + 2O + H]$^+$. The neutral loss of FA 18:2 is shifted by 31.99 Da, indicating the addition of two oxygen atoms. **(B)** MS/MS of di-oxidized, functionalized PLP [PLP + 2O + 3-acpy + H]$^+$.

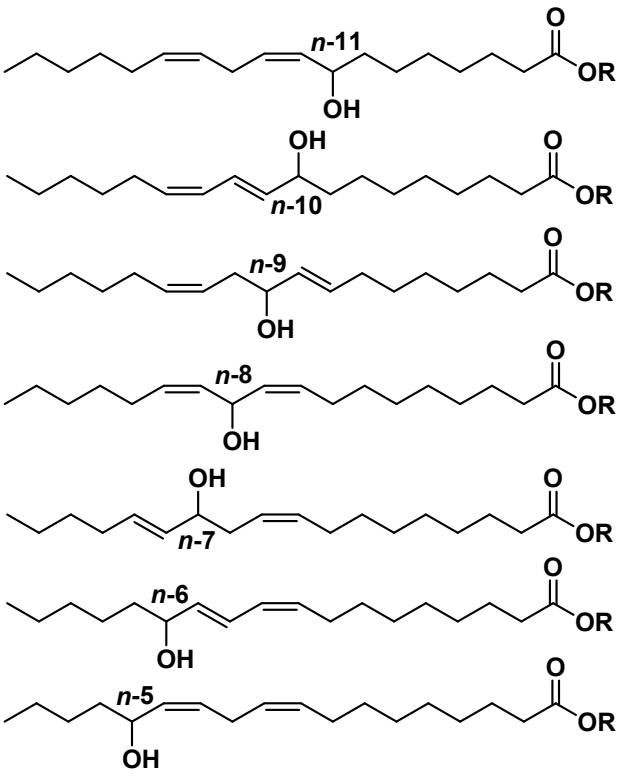

Figure S20. Potential structures of oxidized PLP assuming that oxidation only takes place in allylic positions with respect to C=C bonds. “R” denotes the glycerol backbone containing two FA 16:0 moieties.

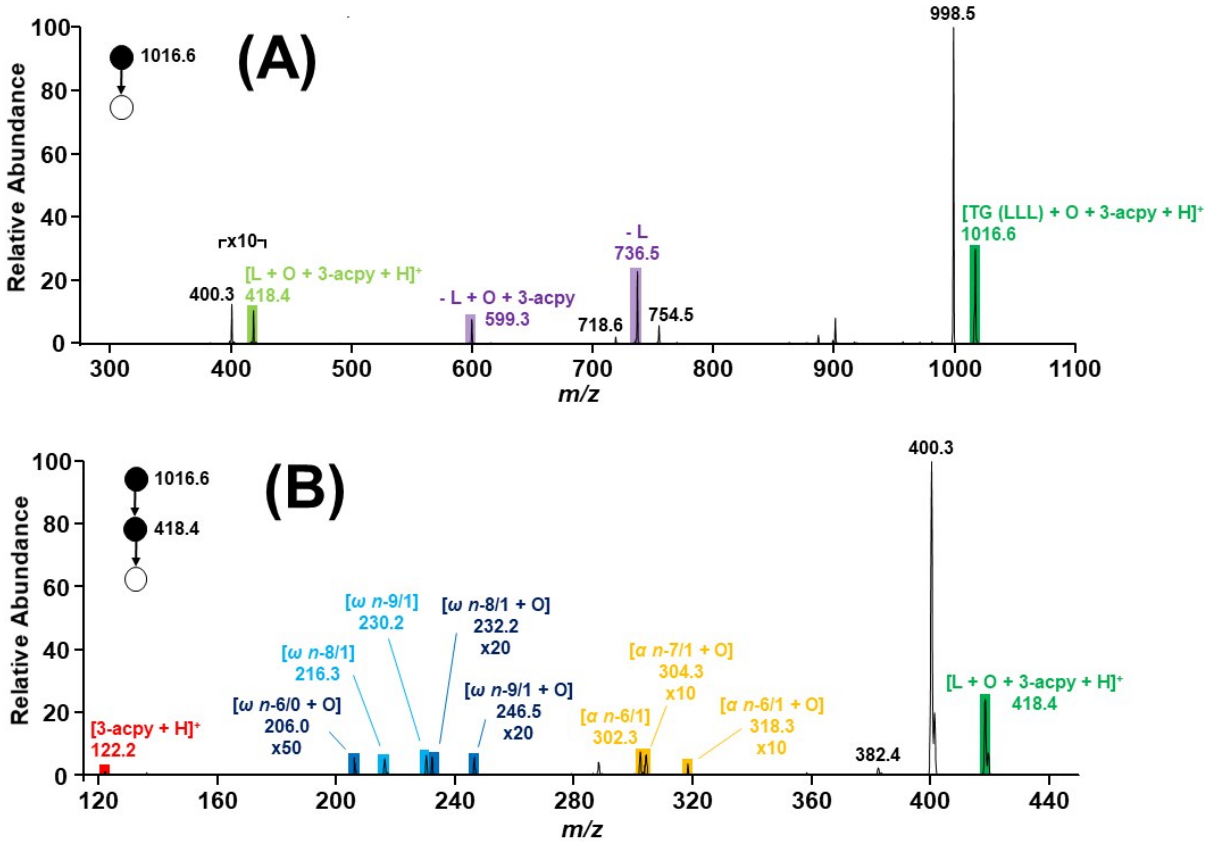

Figure S21. (A) CID-MS^2-spectrum of PB-functionalized, monooxidized TG (LLL). (B) CID-MS^3-spectrum of [L + O + 3-acpy + H]$^+$, liberated upon fragmentation of PB-functionalized, monooxidized TG (LLL).

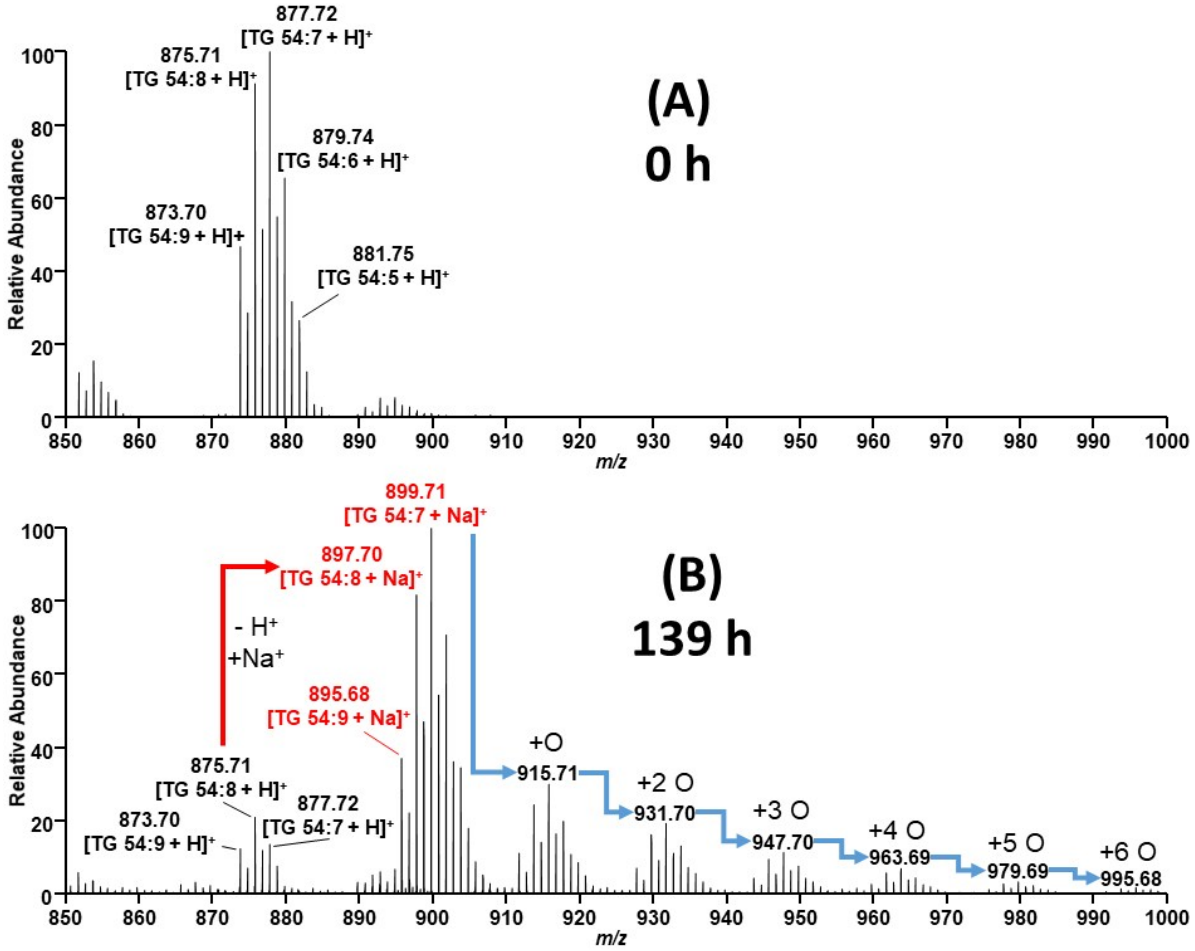

Figure S22. (A) Overview mass spectrum of non-oxidized Sacha Inchi-oil. The signals from *m/z* 873.70 to 881.75 are attributed to $[TG\ 54:9 + H]^+$ to $[TG\ 54:4 + H]^+$. **(B)** Overview mass spectrum of Sacha Inchi-oil that was stored under ambient conditions for 139 h. The attachment of sodium can be observed causing the signals around *m/z* 897.70 (red arrow) and from these signals on, multiple additions of oxygen were detected, each causing a shift of 15.99 Da (blue arrows).

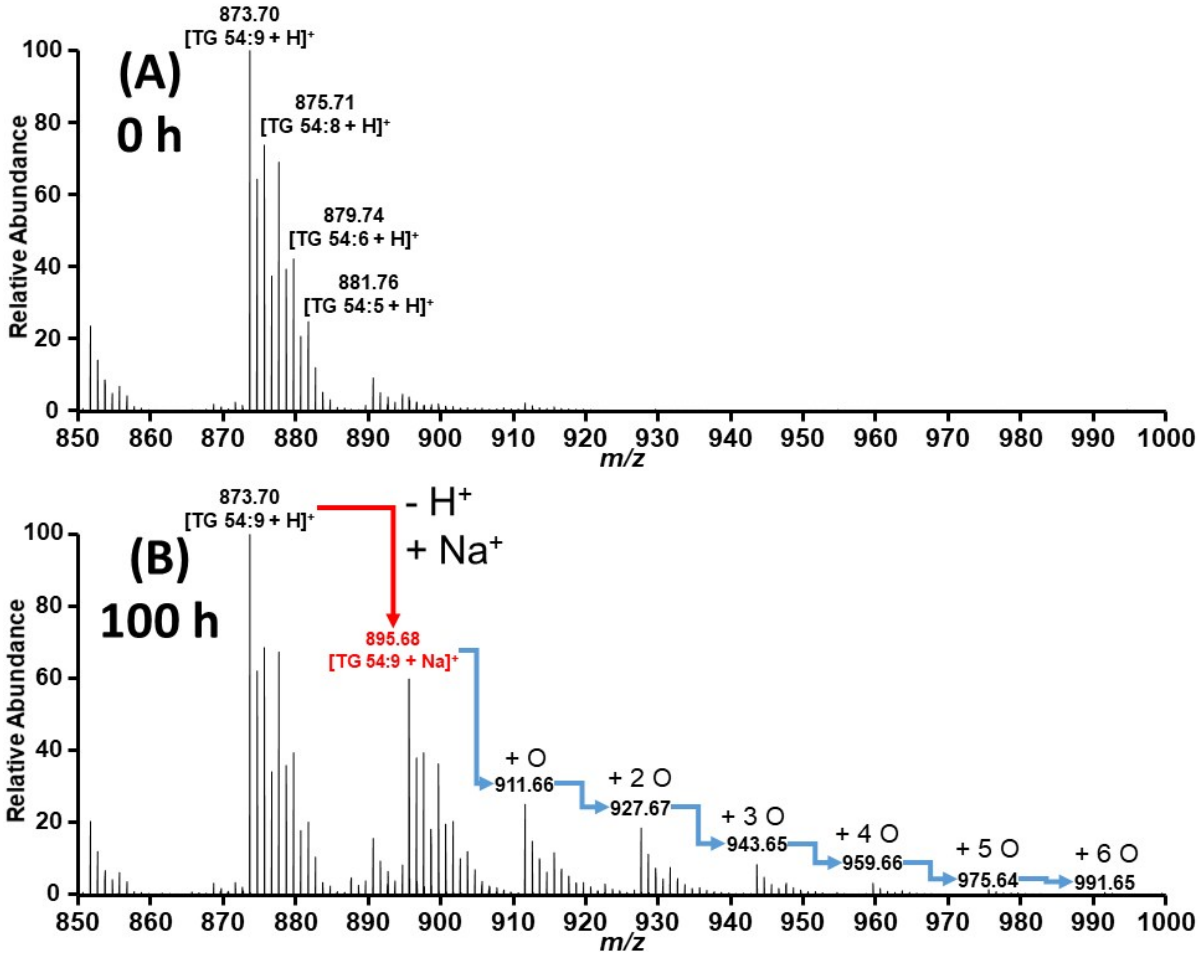

Figure S23. (A) Overview mass spectrum of non-oxidized linseed oil. The signals around *m/z* 873.70 are attributed to $[TG\ 54:9 + H]^+$ to $[TG\ 54:4 + H]^+$. **(B)** Overview mass spectrum of linseed oil that was stored under ambient conditions for 100 h. The attachment of sodium can be observed causing the signals around *m/z* 895.68 (red arrow) and from these signals on, multiple additions of oxygen were detected, each causing a shift of 15.99 Da (blue arrows).

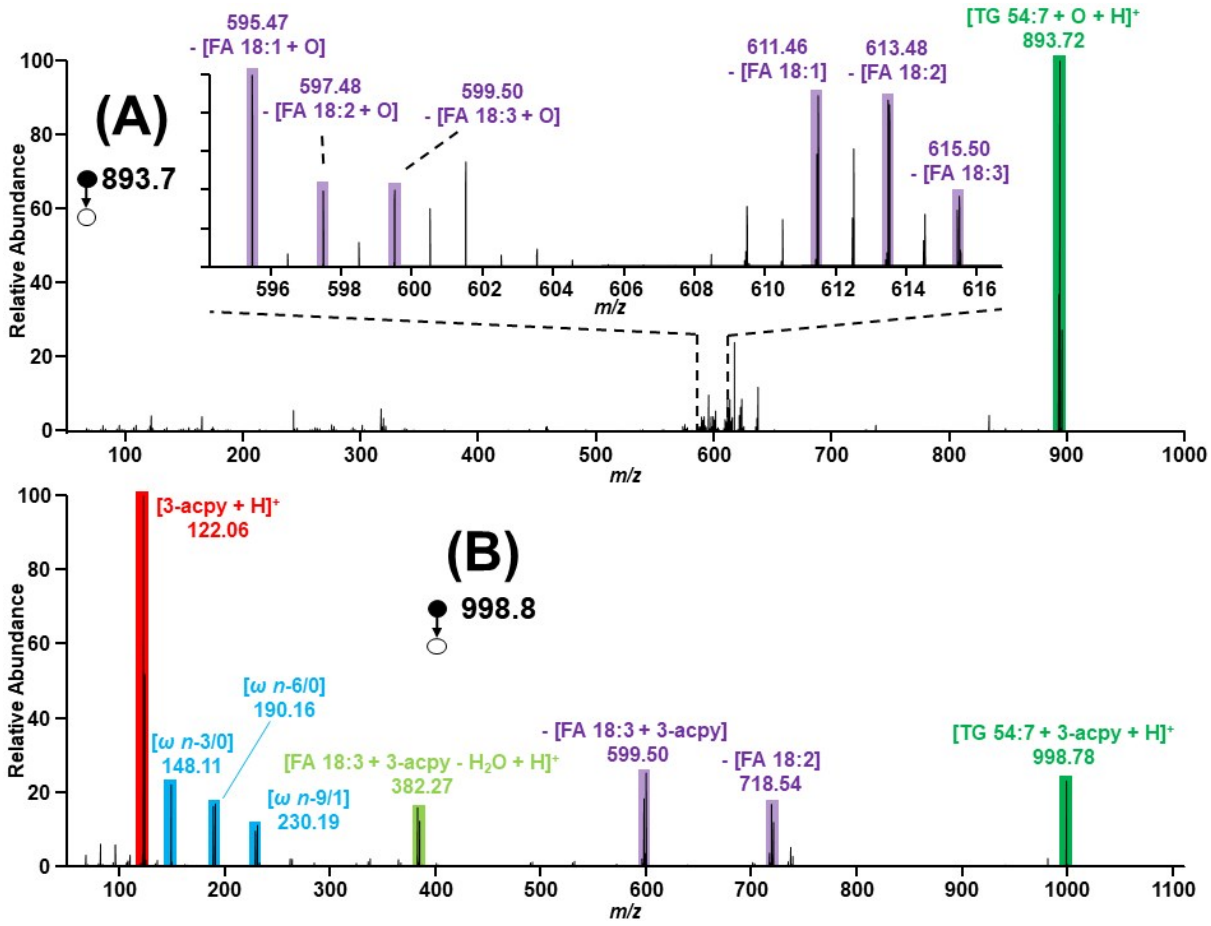

Figure S24. (A) MS/MS spectrum of $[TG\ 54:7 + O + H]^+$ from Sacha Inchi oil. **(B)** PB-MS/MS spectrum of $[TG\ 54:7 + 3\text{-acpy} + H]^+$.

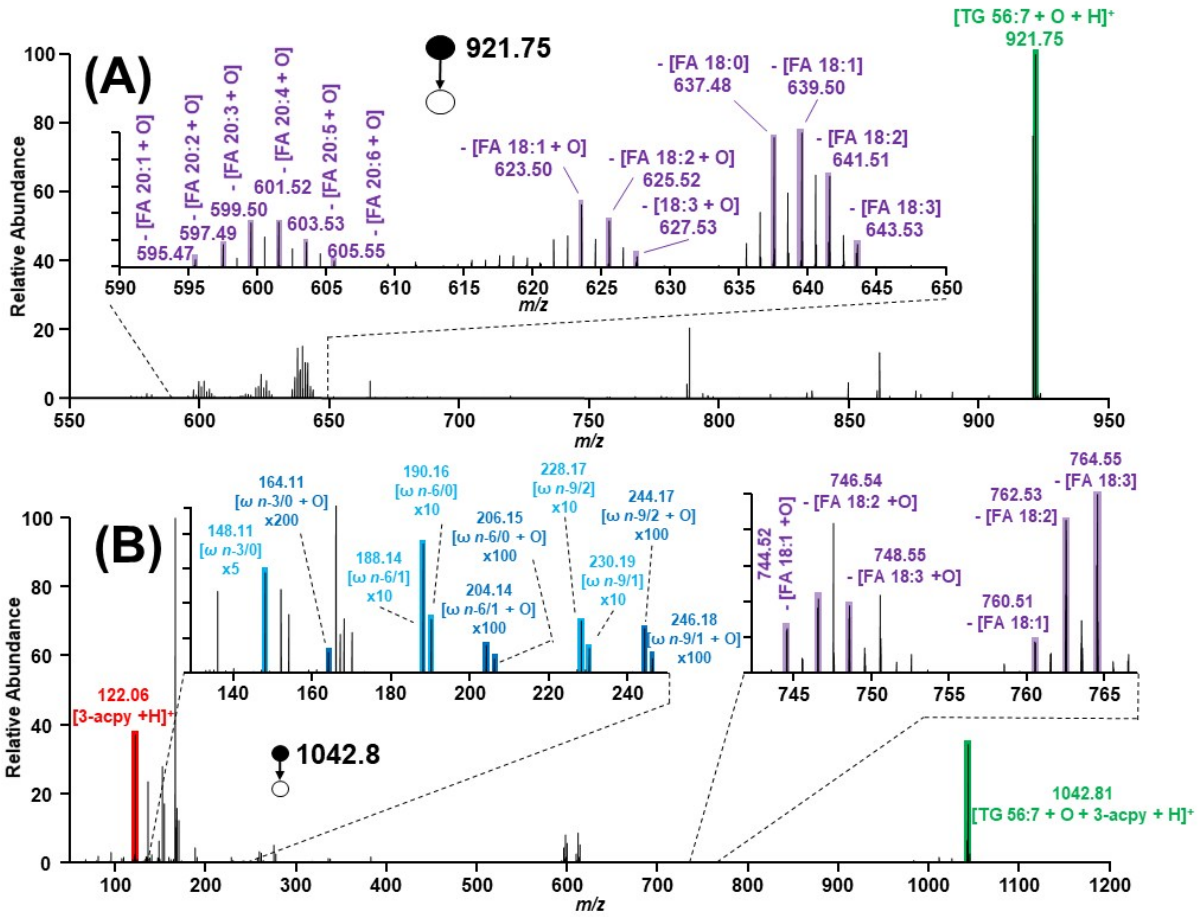

Figure S25. (A) MS/MS spectrum of [TG 56:7 + O + H]$^+$ from oxidized Sacha Inchi oil. The inset shows the signals attributed to neutral losses of oxidized and unoxidized FAs. **(B)** PB-MS/MS spectrum of [TG 56:7 + O + 3-acpy + H]$^+$. The insets show signals of the diagnostic [ω]-ions as well as neutral losses of the FAs. [α]-ions were not detected.

Table S1. List of theoretical *m/z* values obtained by PB-MS^2 of oxidized PLP. Black and blue *m/z* values were detected, whereas red *m/z* values were not detected. Light blue *m/z* values indicate retro-PB fragment ions diagnostic for PLP hydroxylation isomers shown in **Figure S17**. The sum of all [ω]-ions have a relative intensity of 99.5%, whereas [α]-ions have a summed relative intensity of 0.5%.

Oxidation site	[α]	*m/z*	Δ / *ppm*	[ω]	*m/z*	Δ / *ppm*
n-11	*n*-6/1 + O	868.70	+ 1.9	*n*-6/0	190.16	+ 1.8
	n-9/0 + O	828.67	-	*n*-9/1	230.19	+ 2.0
n-10	*n*-6/1 + O	868.70	+ 1.9	*n*-6/0	190.16	+ 1.8
	n-8/0 + O	842.69	-	*n*-8/1	216.18	+ 2.2
n-9	*n*-6/1 + O	868.70	+ 1.9	*n*-6/0	190.16	+ 1.8
	n-10/0	798.66	-	*n*-10/1 + O	260.20	+ 1.9
n-8	*n*-6/1 + O	868.70	+ 1.9	*n*-6/0	190.16	+ 1.8
	n-9/0	812.67	+ 1.8	*n*-9/1 + O	246.19	+ 2.5
n-7	*n*-5/1 + O	882.70	-	*n*-5/0	176.14	+ 1.3
	n-9/0	812.67	+ 1.8	*n*-9/1 + O	246.19	+ 2.5
n-6	*n*-7/1	838.69	-	*n*-7/0 + O	220.17	+ 2.1
	n-9/0	812.67	+ 1.8	*n*-9/1 + O	246.19	+ 2.5
n-5	*n*-6/1	852.71	+ 1.7	*n*-6/0 + O	206.15	+ 2.0
	n-9/0	812.67	+ 1.8	*n*-9/1 + O	246.19	+ 2.5

Table S2. Experimental and theoretical *m/z* values for fragments found in the PB-MS/MS spectrum of $[TG\ 54:7 + O + 3\text{-acpy} + H]^+$ from Sacha Inchi oil.

Fragment type	Sum Formula	Experimental mass / *m/z*	Exact mass / *m/z*	Δ / ppm
[ω *n*-3/0]	$C_{10}H_{14}N^+$	148.1120	148.1121	- 0.7
[ω *n*-4/0]	$C_{11}H_{16}N^+$	162.1278	162.1277	+ 0.6
[ω *n*-5/0]	$C_{12}H_{18}N^+$	176.1435	176.1434	+ 0.6
[ω *n*-6/0]	$C_{13}H_{20}N^+$	190.1589	190.1590	- 0.5
[ω *n*-7/0]	$C_{14}H_{22}N^+$	204.1741	204.1747	- 2.9
[ω *n*-8/0]	$C_{15}H_{24}N^+$	218.1896	218.1903	- 3.2
[ω *n*-9/0]	$C_{16}H_{26}N^+$	232.2056	232.206	- 1.7
[ω *n*-3/0 + O]	$C_{10}H_{14}NO^+$	164.1070	164.1070	± 0.0
[ω *n*-4/0 + O]	$C_{11}H_{16}NO^+$	178.1228	178.1226	+ 1.1
[ω *n*-5/0 + O]	$C_{12}H_{18}NO^+$	192.1377	192.1383	- 3.1
[ω *n*-6/0 + O]	$C_{13}H_{20}NO^+$	206.1533	206.1539	- 2.9
[ω *n*-7/0 + O]	$C_{14}H_{22}NO^+$	220.1688	220.1696	- 3.6
[ω *n*-8/0 + O]	$C_{15}H_{24}NO^+$	234.1845	234.1852	- 3.0
[ω *n*-9/0 + O]	$C_{16}H_{26}NO^+$	248.2001	248.2009	- 3.2
[ω *n*-10/0 + O]	$C_{17}H_{28}NO^+$	262.2159	262.2165	- 2.3
[ω *n*-3/1]	$C_{10}H_{12}N^+$	146.0967	146.0964	+2.1
[ω *n*-4/1]	$C_{11}H_{14}N^+$	160.1122	160.1121	+ 0.6
[ω *n*-5/1]	$C_{12}H_{16}N^+$	174.1272	174.1277	- 2.9
[ω *n*-6/1]	$C_{13}H_{18}N^+$	188.1433	188.1434	- 0.5
[ω *n*-7/1]	$C_{14}H_{20}N^+$	202.1583	202.1590	- 3.5
[ω *n*-8/1]	$C_{15}H_{22}N^+$	216.174	216.1747	- 3.2
[ω *n*-9/1]	$C_{16}H_{24}N^+$	230.1902	230.1903	- 0.4
[ω *n*-10/1]	$C_{17}H_{26}N^+$	244.2051	244.2060	- 3.7
[ω *n*-3/1 + O]	$C_{10}H_{12}NO^+$	162.0915	162.0913	+ 1.2
[ω *n*-4/1 + O]	$C_{11}H_{14}NO^+$	176.1071	176.1070	+ 0.6
[ω *n*-5/1 + O]	$C_{12}H_{16}NO^+$	190.1224	190.1226	- 1.1
[ω *n*-6/1 + O]	$C_{13}H_{18}NO^+$	204.1377	204.1383	- 2.9
[ω *n*-7/1 + O]	$C_{14}H_{20}NO^+$	218.1533	218.1539	- 2.8
[ω *n*-8/1 + O]	$C_{15}H_{22}NO^+$	232.1689	232.1696	- 3.0
[ω *n*-9/1 + O]	$C_{16}H_{24}NO^+$	246.1845	246.1852	- 2.8
[ω *n*-10/1 + O]	$C_{17}H_{26}NO^+$	260.2000	260.2009	- 3.5

Fragment type	Sum Formula	Experimental mass / *m/z*	Exact mass / *m/z*	Δ / ppm
[α *n*-3/6]	$C_{61}H_{98}NO_7^+$	956.7365	956.7338	+ 2.8
[α *n*-4/6]	$C_{60}H_{96}NO_7^+$	942.7142	942.7181	- 4.1
[α n-5/6]	$C_{59}H_{94}NO_7^+$	928.7030	928.7025	+ 0.5
[α *n*-6/6]	$C_{58}H_{92}NO_7^+$	914.6877	914.6868	+ 1.0
[α *n*-7/6]	$C_{57}H_{90}NO_7^+$	900.6711	900.6712	- 0.1
[α *n*-8/6]	$C_{56}H_{88}NO_7^+$	886.6556	886.6555	+ 0.1
[α *n*-9/6]	$C_{55}H_{86}NO_7^+$	872.6404	872.6399	+ 0.6
[α *n*-10/6]	$C_{54}H_{84}NO_7^+$	858.6236	858.6242	- 0.7
[α *n*-3/6 + O]	$C_{61}H_{98}NO_8^+$	972.7288	972.7287	+ 0.1
[α *n*-4/6 + O]	$C_{60}H_{96}NO_8^+$	958.7121	958.7130	- 0.9
[α *n*-5/6 + O]	$C_{59}H_{94}NO_8^+$	944.6980	944.6974	+ 0.6
[α *n*-6/6 + O]	$C_{58}H_{92}NO_8^+$	930.6827	930.6817	+ 1.1
[α *n*-7/6 + O]	$C_{57}H_{90}NO_8^+$	916.6655	916.6661	- 0.7
[α *n*-8/6 + O]	$C_{56}H_{88}NO_8^+$	902.6508	902.6504	+ 0.4
[α *n*-9/6 + O]	$C_{55}H_{86}NO_8^+$	888.6360	888.6348	+ 1.4
[α *n*-10/6 + O]	$C_{54}H_{84}NO_8^+$	874.6179	874.6191	- 1.4
[α *n*-3/5]	$C_{61}H_{100}NO_7^+$	958.7524	958.7494	+ 3.1
[α *n*-4/5]	$C_{60}H_{98}NO_7^+$	944.7358	944.7338	+ 2.1
[α *n*-5/5]	$C_{59}H_{96}NO_7^+$	-	930.7181	-
[α *n*-6/5]	$C_{58}H_{94}NO_7^+$	916.7040	916.7025	+ 1.6
[α *n*-7/5]	$C_{57}H_{92}NO_7^+$	-	902.6868	-
[α *n*-8/5]	$C_{56}H_{90}NO_7^+$	888.6719	888.6712	+ 0.8
[α *n*-9/5]	$C_{55}H_{88}NO_7^+$	874.6564	874.6555	+ 1.0
[α *n*-10/5]	$C_{54}H_{86}NO_7^+$	860.6400	860.6399	+ 0.1